# The Major-Element Composition of Mercury's Surface from MESSENGER X-ray Spectrometry

Larry R. Nittler,[1]* Richard D. Starr,[2] Shoshana Z. Weider,[1] Timothy J. McCoy,[3] William V. Boynton,[4] Denton S. Ebel,[5] Carolyn M. Ernst,[6] Larry G. Evans,[7] John O. Goldsten,[6] David K. Hamara,[4] David J. Lawrence,[6] Ralph L. McNutt Jr.,[6] Charles E. Schlemm II,[6] Sean C. Solomon,[1] Ann L. Sprague[4]

X-ray fluorescence spectra obtained by the MESSENGER spacecraft orbiting Mercury indicate that the planet's surface differs in composition from those of other terrestrial planets. Relatively high Mg/Si and low Al/Si and Ca/Si ratios rule out a lunarlike feldspar-rich crust. The sulfur abundance is at least 10 times higher than that of the silicate portion of Earth or the Moon, and this observation, together with a low surface Fe abundance, supports the view that Mercury formed from highly reduced precursor materials, perhaps akin to enstatite chondrite meteorites or anhydrous cometary dust particles. Low Fe and Ti abundances do not support the proposal that opaque oxides of these elements contribute substantially to Mercury's low and variable surface reflectance.

Elemental abundances at the surface of a rocky planet reflect the composition of the original materials from which the planet formed, as well as the accretion, differentiation, impact, and geological processes that have shaped the surface over billions of years. Before the MESSENGER mission (*1*), constraints on the composition of Mercury were indirect and included a high overall metal/silicate ratio (inferred from the planet's bulk density), low FeO in surface silicates, and the presence of K, Na, Ca, and other elements in the planet's exosphere (*2*–*5*). Several models of Mercury's origin and early evolution were developed to explain the high metal/silicate ratio, including sorting of metal and silicate particles in the early solar nebula by thermal or physical processes before planetary accretion (*6*, *7*), evaporation of an outer silicate crust and mantle by a hot early solar nebula (*8*), and removal of large portions of the outer silicate fraction of a differentiated planet by a giant impact (*9*, *10*). These models led to a variety of predictions for the composition of surface materials on Mercury (*11*). The MErcury Surface, Space ENvironment, GEochemistry, and Ranging (MESSENGER) spacecraft, in orbit around Mercury since 18 March 2011, includes an X-Ray Spectrometer (XRS), which makes direct measurements of the surface abundances of the key rock-forming elements: Mg, Al, Si, S, Ca, Ti, and Fe. Here, we discuss XRS observations of Mercury's surface chemistry from the first 90 days of MESSENGER orbital science operations.

The MESSENGER XRS (*12*, *13*) detects fluorescent x-ray emissions, induced by solar x-rays, from the top tens of micrometers of Mercury's surface. It consists of three planet-facing gas-filled proportional counters (GPCs), which detect fluorescent and scattered solar x-rays with energies of 1 to 10 keV. Thin foils of Mg and Al in front of two of the detectors allow deconvolution of the fluorescent signals from the geochemically important elements Mg, Al, and Si. Spatial resolution for a single spectral measurement depends on spacecraft altitude and integration time and ranges from <50 km to >3000 km (*13*).

The solar x-ray spectrum is highly variable in time, strongly affecting the strength and shape of x-ray spectra observed from Mercury's surface. The XRS thus also includes a Sun-facing detector (Solar Assembly for X-rays, or SAX) to simultaneously measure incident solar x-ray spectra (*12*). During typical solar conditions, XRS detects fluorescent signals only from Mg, Al, and Si. However, the solar flux is greatly enhanced during flares, especially at higher energies, allowing detection of elements with atomic numbers up to that of Fe. Here, we focus on data acquired during solar flares because these provide the most geochemical information.

We used a forward modeling approach to convert observed spectra to elemental abundances (*13*). For a given observation, a theoretical solar plasma spectrum was fit to the observed SAX spectrum and used, along with the appropriate observation geometry (incidence, emission, and phase angles) and an assumed composition, to calculate theoretical XRS spectra (*13*–*15*). Elemental abundances were varied in a nonlinear least-squares fitting procedure until the best match to the observed spectra was obtained. We discuss abundance ratios relative to silicon because these are more accurately determined than absolute abundances.

Most of the data reported here (Table 1) were acquired at high altitude, when the instrument's field of view projected onto the planet's surface (or its footprint) was large, and hence represent averages over large areas of the surface (Fig. 1). The measured footprints are primarily located in the southern hemisphere, between longitudes of about −180° and −60°E. Low-altitude data from one flare (on 16 April 2011) have smaller footprints and include one region of northern volcanic smooth plains (*16*).

Mercury has a higher Mg/Si ratio and lower Al/Si and Ca/Si ratios than the terrestrial and lunar crusts (Fig. 2), indicating a lower abundance of plagioclase feldspar, a common crustal mineral. Mercury's ratios are intermediate between typical basaltic compositions and more ultramafic compositions comparable to terrestrial komatiites. The derived compositions are reasonably close to those estimated from mineral assemblages inferred from ground-based infrared spectral data (*17*, *18*).

All analyzed flare spectra unambiguously show the presence of abundant sulfur. The S/Si ratios range from ~0.05 to 0.15. An O abundance inferred from the usual stoichiometry of the major cations implies an average surface Si abundance of ~25 weight % (wt %) and hence an S abundance of up to ~4 wt % in surface materials. This concentration is much higher than observed in the bulk silicate Earth, lunar silicates, or stony meteorites from Mars and differentiated asteroids, the S content for all of which are estimated to be $\lesssim 0.2$ wt %. The low S abundances on these objects are thought to reflect loss of volatiles during planet formation and/or sequestration into planetary cores. Higher S abundances, comparable to those reported here, have been measured in situ on the surfaces of Mars and Venus, but those instances likely are the result of aqueous processing and surface-atmospheric interaction, respectively (*19*, *20*).

Data from the most intense flares (*13*) reveal that Mercury's surface is low in Ti and Fe. Derived Ti/Si ratios range from 0.007 to 0.03, and Fe/Si ratios range from 0.01 to 0.15, giving upper limits on absolute abundances of ~0.8 wt % for Ti and ~4 wt % for Fe. Analysis of the highest signal-to-noise XRS spectra also provided upper limits of ~0.2% for Cl and ~0.5 wt % for Cr and Mn (*13*).

Mercury's relatively low Al/Si and Ca/Si ratios rule out the presence of a plagioclase-rich crust similar to that of the lunar highlands. The latter is thought to have formed by flotation of crystallized plagioclase-rich rocks that solidified

---

[1] Department of Terrestrial Magnetism, Carnegie Institution of Washington, Washington, DC 20015, USA. [2] Physics Department, The Catholic University of America, Washington, DC 20064, USA. [3] Smithsonian Institution, Washington, DC 20013, USA. [4] Lunar and Planetary Laboratory, University of Arizona, Tucson, AZ 85721, USA. [5] Department of Earth and Planetary Science, American Museum of Natural History, New York, NY 10024, USA. [6] The Johns Hopkins University Applied Physics Laboratory, Laurel, MD 20723, USA. [7] Computer Sciences Corporation, Lanham-Seabrook, MD 20706, USA.

*To whom correspondence should be addressed. E-mail: lnittler@ciw.edu

**Table 1.** Elemental abundances derived for Mercury's surface from XRS observations during 10 solar flares. The flare on 16 April was divided into two time segments for independent analysis (nos. 1 and 2). Mg/Si, Al/Si, S/Si, and Ca/Si ratios are means and standard deviations of individual integrations for each flare. Errors incorporate systematic errors due to uncertain solar spectra fitting. Ti/Si and Fe/Si are derived ratios and statistical errors for highest signal-to-noise spectrum for a given flare. The second segment of the 16 April flare was analyzed as a single summed spectrum; derived ratios and statistical errors are shown.

| Flare no. | Date and start time (UTC) | Total integration time (s) | Max. solar temp. ($10^6$ K) | Mg/Si | Al/Si | S/Si | Ca/Si | Ti/Si | Fe/Si |
|---|---|---|---|---|---|---|---|---|---|
| 1 | 16 April 2011<br>16:40:41 | 705 | 13.2 | 0.62 ± 0.04 | 0.19 ± 0.03 | 0.14 ± 0.02 | 0.30 ± 0.06 | | |
| 2 | 16 April 2011<br>16:53:06 | 80 | 8.6 | 0.33 ± 0.03 | 0.22 ± 0.05 | 0.08 ± 0.02 | | | |
| 3 | 22 April 2011<br>1:26:13 | 3600 | 11.5 | 0.50 ± 0.07 | 0.24 ± 0.02 | 0.09 ± 0.01 | 0.20 ± 0.04 | | |
| 4 | 22 April 2011<br>4:56:47 | 2319 | 17.3 | 0.58 ± 0.04 | 0.17 ± 0.02 | 0.15 ± 0.02 | 0.29 ± 0.03 | <0.01 | 0.03 ± 0.02 |
| 5 | 22 April 2011<br>17:01:00 | 909 | 14.6 | 0.67 ± 0.08 | 0.18 ± 0.01 | 0.15 ± 0.01 | 0.30 ± 0.03 | 0.010 ± 0.004 | 0.06 ± 0.01 |
| 6 | 1 May 2011<br>23:22:43 | 900 | 16.1 | 0.41 ± 0.03 | 0.25 ± 0.005 | 0.07 ± 0.01 | 0.21 ± 0.003 | 0.007 ± 0.003 | 0.12 ± 0.01 |
| 7 | 15 May 2011<br>23:24:02 | 2250 | 13.4 | 0.43 ± 0.09 | 0.28 ± 0.03 | 0.07 ± 0.005 | 0.22 ± 0.01 | 0.03 ± 0.01 | 0.15 ± 0.01 |
| 8 | 13 June 2011<br>3:53:14 | 900 | 16.5 | 0.39 ± 0.04 | 0.26 ± 0.004 | 0.05 ± 0.002 | 0.15 ± 0.01 | 0.007 ± 0.001 | 0.05 ± 0.01 |
| 9 | 14 June 2011<br>21:44:36 | 2250 | 15.6 | 0.36 ± 0.06 | 0.26 ± 0.01 | 0.06 ± 0.01 | 0.18 ± 0.01 | | |
| 10 | 16 June 2011<br>10:19:05 | 2250 | 14.2 | 0.53 ± 0.03 | 0.27 ± 0.004 | 0.07 ± 0.01 | 0.17 ± 0.02 | <0.01 | 0.08 ± 0.01 |
| 11 | 16 June 2011<br>11:56:46 | 800 | 11.8 | 0.64 ± 0.06 | 0.28 ± 0.02 | 0.07 ± 0.01 | 0.18 ± 0.02 | | |

from a global magma ocean (*21*). It is not known whether Mercury also experienced a magma ocean stage in its early history. Magma ocean models [e.g., (*21*, *22*)] predict that the formation of a flotation crust depends strongly on the planet's bulk silicate composition. For FeO abundances less than a few percent in the bulk silicate fraction of the planet, crystallizing plagioclase will not float in the coexisting magma. In such a case, the final surface composition would likely be dominated by lava flows formed from the subsequent partial melting of mantle material solidified during magma ocean cooling. The low surface Fe abundance as measured by XRS confirms a low total FeO abundance in Mercury's mantle (*23*) and therefore suggests that a plagioclase flotation crust never formed. The observed compositions are also inconsistent with some predictions (*22*) for remelting of magma ocean solidification products (Fig. 2), but only a limited set of starting compositions has been considered in these models to date.

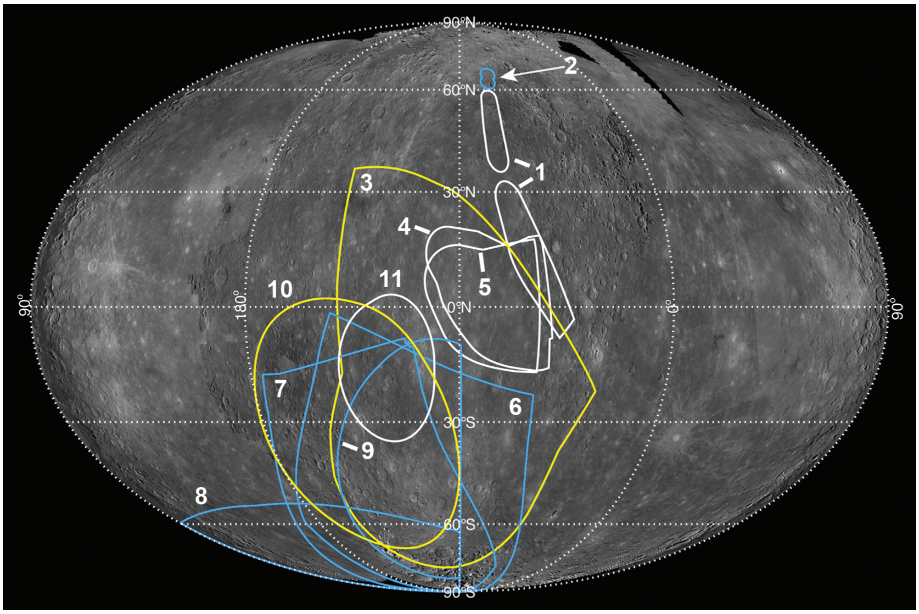

**Fig. 1.** Regions of Mercury (footprints) sampled by XRS during analyzed flares, numbered according to Table 1. Outline colors reflect derived Mg/Si ratios: white, Mg/Si ≈ 0.6; yellow, Mg/Si ≈ 0.5; blue, Mg/Si ≈ 0.4. Arrow indicates spatially resolved measurement of a portion of northern plains material (*16*).

The derived Mg/Si, Al/Si, and Ca/Si ratios indicate a surface composition depleted in plagioclase relative to compositions characteristic of early melts from an Earth-like mantle (e.g., oceanic basalts). This result might suggest removal of an early basaltic crust by either large-scale evaporation (*8*) or giant impact events (*9*, *10*). However, neither model is supported by mounting evidence that Mercury is not highly depleted in volatile elements relative to the other terrestrial planets (*24*). A more likely scenario is that Mercury's unusual metal-rich, FeO-poor composition reflects the primary nature of its precursor materials. Early hypotheses (*6*) that Mercury formed primarily from high-temperature materials that condensed at equilibrium in the innermost solar system predicted high abundances of refractory elements such as Ca and Al and low abundances of volatile elements such as S and K. Such refractory-rich, volatile-poor compositions are ruled out by the elemental

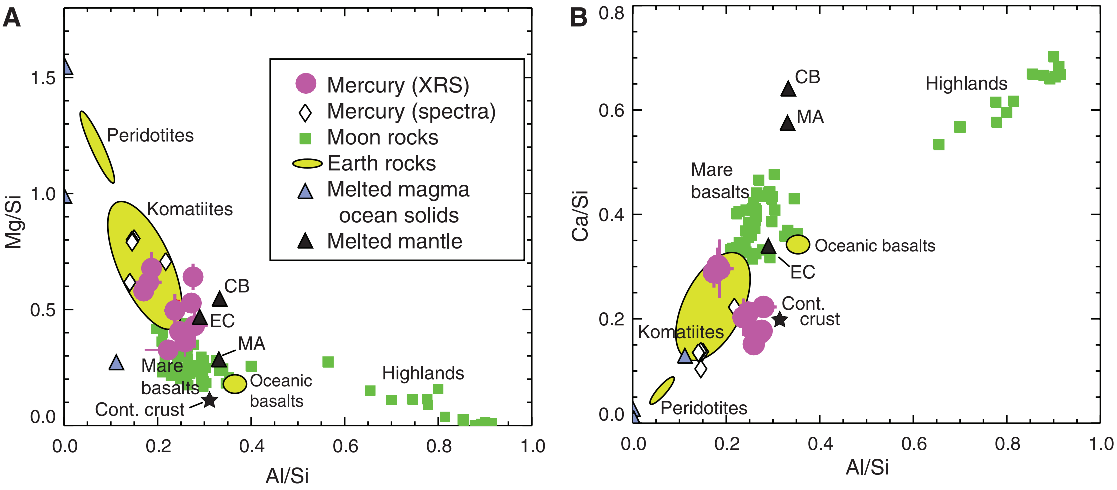

**Fig. 2.** (**A** and **B**) Mg/Si, Al/Si, and Ca/Si mass ratios for Mercury (Table 1) compared with terrestrial (*35*) and lunar (*36*) compositions and predicted Mercury compositions. Mercury (spectra) denotes compositions inferred from ground-based infrared spectra (*17*, *18*). Also shown are predictions of partially melted magma ocean products (*22*), partially melted CB chondrite composition (*11*), partially melted EC (*26*, *27*), and partial melts (*11*) from a mix of refractory and volatile materials (MA) (*25*).

abundances reported here. More recent ideas focus on accreting Mercury from mixtures of refractory-enriched and Earth-like compositions (*11*, *25*) or highly reduced (*26*) and/or metal-rich (*22*) chondritic meteorite compositions (enstatite and/or CB chondrites, respectively). We compared the XRS results with Mg/Si, Al/Si, and Ca/Si ratios predicted for partial melting of material of these compositions (as proxies for surface lava flows) (Fig. 2). Of these compositions, only the partially melted enstatite chondrite (EC) composition is reasonably similar to the observations, although not a perfect match. This composition is also enriched in S (*26*), at about the same level that we observe on Mercury. This is because, under highly reducing conditions, substantial S is incorporated into silicate melts (*27*), unlike the situation under more oxidizing conditions.

The low Fe abundance indicates that the surface S cannot be present primarily in the form of iron sulfides. More likely the S occurs in Mg- and/or Ca-rich sulfides, which are stable under reducing conditions and present in highly reduced enstatite chondrite and aubrite meteorites. Their presence on Mercury has been previously suggested on the basis of ground-based observations (*28*) and is supported by a general correlation among Mg/Si, Ca/Si, and S/Si ratios observed here (*13*) (fig. S8). Magmas coexisting with these sulfides would have extremely low FeO contents (<1 wt %) (*25*). Moreover, the high abundance of S, if it can be extrapolated to Mercury's interior, could potentially provide an abundant source of volatile gases to drive pyroclastic volcanism on Mercury (*29*, *30*).

Mercury's geologic evolution has shaped a surface that likely contains materials varying in composition and depths of origin (*31*, *32*). It is therefore unrealistic to expect the surface composition to match precisely the predictions of a single-stage episode of partial melting from a primitive mantle. Nonetheless, the similarity of the observed average composition to that predicted by simple partial melting of an EC-like composition, especially the high S abundance, strongly suggests that Mercury indeed formed preferentially from highly reduced, but not strongly volatile-depleted, precursors. However, ECs have insufficiently high bulk Fe/Si ratios to explain Mercury's high density without an additional step of metal/silicate fractionation in the solar nebula or silicate removal by giant impact. It is also unlikely that the primitive extraterrestrial materials studied today completely sample the range of building blocks from which the terrestrial planets accreted. It is possible that EC-like objects with higher metal abundances were present in the early inner solar system. Alternatively, Mercury may have been built from solids condensed in ice-poor systems enriched in anhydrous interplanetary dust particles (*33*). These particles, likely derived from comets, are also highly reduced.

Data acquired by MESSENGER during its three flybys of Mercury in 2008–2009 revealed the presence of distinct terrains with subtle differences in color and reflectance that are suggestive of differing chemical compositions (*28*, *29*). In particular, color and reflectance observations have been interpreted in terms of a variable contribution from comparatively dark, spectrally neutral material, and suggested candidate opaque minerals include Fe- and Ti-bearing oxides and/or sulfides. Moreover, flyby data from MESSENGER's Neutron Spectrometer (*34*) indicate a neutron-absorption cross section similar to that of several lunar mare soils, for which the neutron absorption is dominated by a combination of Fe and Ti. This result supported the suggestion that Fe-Ti oxides may be in high abundance on Mercury, despite the low amount of FeO in the surface silicates. The low Fe and Ti abundances inferred from the XRS data, however, do not support a high abundance of such oxides on the surface and require that additional element(s) are responsible for the high observed neutron-absorption cross section. Observed abundances or abundance limits on S, Fe, Cl, Ti, and/or Mn are consistent with the lower limit of the neutron absorption (*13*). Trace amounts of Sm and Gd, which have extremely high neutron-absorption cross sections, may also be present. Although the large size of most of the XRS footprints on Mercury's surface makes direct correlation of the present results with identified geological units difficult, we note that the highest Mg/Si, Ca/Si, and S/Si ratios are found in areas that include substantial amounts of low-reflectance material, supporting the possibility that sulfides contribute to the low reflectance.

## References and Notes

1. S. C. Solomon *et al.*, *Planet. Space Sci.* **49**, 1445 (2001).
2. H. T. Howard *et al.*, *Science* **185**, 179 (1974).
3. D. M. Hunten, D. E. Shemansky, T. H. Morgan, C. R. Chapman, M. S. Matthews, "The Mercury atmosphere," in *Mercury*, F. Vilas, C. R. Chapman, M. S. Matthews, Eds. (Univ. Arizona Press, Tucson, AZ, 1988), pp. 562–612.
4. S. C. Solomon, *Earth Planet. Sci. Lett.* **216**, 441 (2003).
5. B. W. Denevi, M. S. Robinson, *Icarus* **197**, 239 (2008).
6. J. S. Lewis, *Annu. Rev. Phys. Chem.* **24**, 339 (1973).
7. S. J. Weidenschilling, *Icarus* **35**, 99 (1978).
8. B. Fegley Jr., A. G. W. Cameron, *Earth Planet. Sci. Lett.* **82**, 207 (1987).
9. W. W. L. Benz, W. L. Slattery, A. G. W. Cameron, *Icarus* **74**, 516 (1988).
10. W. Benz, A. Anic, J. Horner, J. A. Whitby, *Space Sci. Rev.* **132**, 189 (2007).
11. G. J. Taylor, E. R. D. Scott, in *Meteorites, Comets, and Planets*, A. M. Davis, Ed., vol. 1 of *Treatise on Geochemistry*, H. D. Holland, K. K. Turekian, Eds. (Elsevier-Pergamon, Oxford, UK, 2003), pp. 477–485.
12. C. E. Schlemm II *et al.*, *Space Sci. Rev.* **131**, 393 (2007).
13. Details of analysis methods are available as supporting material on *Science* Online.
14. P. E. Clark, J. I. Trombka, *J. Geophys. Res.* **102**, 16361 (1997).
15. L. R. Nittler *et al.*, *Meteorit. Planet. Sci.* **36**, 1673 (2001).
16. J. W. Head *et al.*, *Science* **333**, 1853 (2011).
17. A. L. Sprague *et al.*, *Planet. Space Sci.* **57**, 364 (2009).
18. P. Wurz *et al.*, *Planet. Space Sci.* **58**, 1599 (2010).
19. R. Rieder *et al.*, *Science* **278**, 1771 (1997).
20. B. Fegley Jr., in *Meteorites, Comets, and Planets*, A. M. Davis, Ed., vol. 1 of *Treatise on Geochemistry*, H. D. Holland, K. K. Turekian, Eds. (Elsevier-Pergamon, Oxford, UK, 2003), pp. 487–507.
21. P. H. Warren, *Annu. Rev. Earth Planet. Sci.* **13**, 201 (1985).

22. S. M. Brown, L. T. Elkins-Tanton, *Earth Planet. Sci. Lett.* **286**, 446 (2009).
23. M. S. Robinson, G. J. Taylor, *Meteorit. Planet. Sci.* **36**, 841 (2001).
24. P. N. Peplowski *et al.*, *Science* **333**, 1850 (2011).
25. J. W. Morgan, E. Anders, *Proc. Natl. Acad. Sci. U.S.A.* **77**, 6973 (1980).
26. T. H. Burbine *et al.*, *Meteorit. Planet. Sci.* **37**, 1233 (2002).
27. T. J. McCoy, T. L. Dickinson, G. E. Lofgren, *Meteorit. Planet. Sci.* **34**, 735 (1999).
28. A. L. Sprague, D. M. Hunten, K. Lodders, *Icarus* **118**, 211 (1995).
29. L. Kerber *et al.*, *Earth Planet. Sci. Lett.* **285**, 263 (2009).
30. D. T. Blewett *et al.*, *Science* **333**, 1856 (2011).
31. B. W. Denevi *et al.*, *Science* **324**, 613 (2009).
32. M. S. Robinson *et al.*, *Science* **321**, 66 (2008).
33. D. S. Ebel, C. M. O'D. Alexander, *Planet. Space Sci.*, 10.1016/j.pss.2011.07.017 (2011).
34. D. J. Lawrence *et al.*, *Icarus* **209**, 195 (2010).
35. K. Lodders, B. Fegley, *The Planetary Scientist's Companion* (Oxford Univ. Press, New York, 1998).
36. J. J. Papike, G. Ryder, C. K. Shearer, in *Planetary Materials*, J. J. Papike, Ed., vol. 36 of *Reviews in Mineralogy*, P. H. Ribbe, Ed. (Mineralogical Society of America, Washington, DC, 1998), pp. 5-1–5-234.

**Acknowledgments:** We thank the MESSENGER team for the development, cruise, orbit insertion, and Mercury orbital operations of the MESSENGER spacecraft. The NASA Discovery Program under contract NAS5-97271 to The Johns Hopkins University Applied Physics Laboratory and NASW-00002 to the Carnegie Institution of Washington supports the MESSENGER mission to Mercury. Several of the authors are supported by NASA's MESSENGER Participating Scientist Program.

**Supporting Online Material**
www.sciencemag.org/cgi/content/full/333/6051/1847/DC1
Materials and Methods
SOM Text
Figs. S1 to S8
Table S1
References (*37–60*)

22 July 2011; accepted 31 August 2011
10.1126/science.1211567

---

# Radioactive Elements on Mercury's Surface from MESSENGER: Implications for the Planet's Formation and Evolution

**Patrick N. Peplowski,[1]* Larry G. Evans,[2] Steven A. Hauck II,[3] Timothy J. McCoy,[4] William V. Boynton,[5] Jeffery J. Gillis-Davis,[6] Denton S. Ebel,[7] John O. Goldsten,[1] David K. Hamara,[5] David J. Lawrence,[1] Ralph L. McNutt Jr.,[1] Larry R. Nittler,[8] Sean C. Solomon,[8] Edgar A. Rhodes,[1] Ann L. Sprague,[5] Richard D. Starr,[9] Karen R. Stockstill-Cahill[4]**

The MESSENGER Gamma-Ray Spectrometer measured the average surface abundances of the radioactive elements potassium (K, 1150 ± 220 parts per million), thorium (Th, 220 ± 60 parts per billion), and uranium (U, 90 ± 20 parts per billion) in Mercury's northern hemisphere. The abundance of the moderately volatile element K, relative to Th and U, is inconsistent with physical models for the formation of Mercury requiring extreme heating of the planet or its precursor materials, and supports formation from volatile-containing material comparable to chondritic meteorites. Abundances of K, Th, and U indicate that internal heat production has declined substantially since Mercury's formation, consistent with widespread volcanism shortly after the end of late heavy bombardment 3.8 billion years ago and limited, isolated volcanic activity since.

Measurements of the surface composition of Mercury offer a special window into the epoch of planet formation in the inner solar system. Mercury likely preserves a more complete record of early crustal formation than do Venus, Earth, or Mars, each of which experienced extensive and prolonged resurfacing and near-surface alteration since earliest crustal formation. The MESSENGER spacecraft, inserted into orbit about Mercury on 18 March 2011, carries a suite of instruments designed for elemental and mineralogical remote sensing. We report abundances of radioactive elements on the surface of Mercury that we determined from measurements with MESSENGER's Gamma-Ray Spectrometer (GRS).

The MESSENGER GRS measures 0.25- to 9-MeV gamma rays originating from isotope-specific gamma-ray emission from the surface (*1*). The two sources of gamma-ray emission are natural radioactive decay of unstable elements (e.g., K, Th, U) and excitation of stable elements (e.g., Si, O, Fe, Ti, S, Ca) by incident galactic cosmic rays. This work focuses on measurements of the elemental abundances of K, Th, and U through the detection of gamma rays emitted during the decay of the naturally occurring radioactive isotopes $^{40}$K, $^{232}$Th, and $^{238}$U. MESSENGER's highly eccentric orbit, combined with the altitude dependence of the gamma-ray signal, limits GRS compositional measurements to the region northward of ~20° S latitude. GRS compositional data nonetheless cover a variety of geologic terrain types, including heavily cratered terrain and smooth plains (*2*, *3*). The data discussed here were acquired at low altitudes (<2000 km) during the first Mercury sidereal day (~59 Earth days) of orbital operations (*4*). To improve the statistical significance of the results, the low-altitude data were summed to create a single data set covering the measured region. The resulting GRS measurements of surface elemental abundances therefore should be regarded as representative values for this region.

Count rates of gamma rays emanating from the surface are obtained by fitting the peaks of interest in the gamma-ray energy spectra (Fig. 1) for the summed low-altitude measurements and correcting for the background gamma-ray count rates derived from a summed high-altitude (>14,000 km) data set. These count rates have been compared, for each spectral peak, to count rates in the detector derived from calculated surface gamma-ray fluxes to determine the elemental abundance required to account for the measured signal (*4*). The average surface abundances of radioactive elements on the surface of Mercury north of ~20°S are 1150 ± 220 parts per million (ppm) K, 220 ± 60 parts per billion (ppb) Th, and 90 ± 20 ppb U. The quoted errors represent the 1-SD statistical uncertainties of the measurements, as well as the systematic uncertainties introduced during the conversion of measured count rates to surface elemental abundances.

Ratios of the moderately volatile incompatible element K to the refractory incompatible elements Th and U provide insights into the volatile inventory of planetary bodies. In contrast, the absolute abundances of these elements can vary appreciably over a planetary surface as a result of variations in melt generation and crustal emplacement and modification processes. Mercury's K/Th ratio is 5200 ± 1800, a value comparable to those for the other terrestrial planets, which range from 2000 to 7000 (*5*, *6*). By contrast, the lunar K/Th value (360) is an order of magnitude lower (*7*), indicative of the depletion of lunar volatiles relative to those of Earth. Mercury's K/Th ratio indicates that the planet's volatile budget relative to refractory elements is similar to that of the other terrestrial planets.

---

[1]The Johns Hopkins University Applied Physics Laboratory, Laurel, MD 20723, USA. [2]Computer Sciences Corporation, Lanham-Seabrook, MD 20706, USA. [3]Department of Geological Sciences, Case Western Reserve University, Cleveland, OH 44106, USA. [4]National Museum of Natural History, Smithsonian Institution, Washington, DC 20013, USA. [5]Lunar and Planetary Laboratory, University of Arizona, Tucson, AZ 85721, USA. [6]Hawaii Institute of Geophysics and Planetology, University of Hawaii, Honolulu, HI 98622, USA. [7]Department of Earth and Planetary Science, American Museum of Natural History, New York, NY 10024, USA. [8]Department of Terrestrial Magnetism, Carnegie Institution of Washington, Washington, DC 20015, USA. [9]Physics Department, The Catholic University of America, Washington, DC 20064, USA.

*To whom correspondence should be addressed. E-mail: patrick.peplowski@jhuapl.edu